Performance Optimised Geometry of Railway Crossings
Design and Implementation

Markine, Valeri; Wan, C.

DOI
10.4203/ijrt.5.2.1

Publication date
2016

Document Version
Accepted author manuscript

Published in
The International Journal of Railway Technology

V.L. Markine, C. Wan, "Performance Optimised Geometry of Railway Crossings: Design and Implementation", International Journal of Railway Technology, 5(2), 1-25, 2016. doi:10.4203/ijrt.5.2.1

Performance Optimised Geometry of Railway Crossings: Design and Implementation

V.L. Markine[1] and C. Wan[2]

[1] Delft University of Technology, The Netherlands
[2] Trondheim University of Science and Technology Trondheim, Norway

Abstract

The paper presents an optimisation procedure for improvement of crossing performance by adjusting the cro sing (including the wing rail) geometry. The improvement of the crossing performance is achieved by reducing the normal contact pressure and wear index, while shifting the location of the wheel impact (fatigue area) along the crossing. By shifting the fatigue area the life of the crossing can be prolonged.

To demonstrate the proposed procedure the geometry of a crossing (crossing angle 1:15) has been optimised. The effect of two typical wheel profiles used on the considered crossing is taken in to account during the optimisation. The robustness of the obtained geometries has been verified using the numerical simulations with track geometrical irregularities.

Using the optimisation procedure two improved geometries of the crossing have been obtained. In both designs the normal contact pressure was reduced as compared to the reference design, while the fatigue area in the second crossing was shifted further from the tip point of the crossing as compared to the first crossing. Important is that the second crossing geometry can be obtained from the first crossing simply by grinding.

To implement the new crossing geometry a new measurement device has been proposed. The device can be used for assessment of wear of existing crossings and during adjusting/restoration of the crossing geometry.

Keywords: instrumented turnout, wheel/rail contact, crossing geometry optimisation

V.L. Markine, C. Wan, "Performance Optimised Geometry of Railway Crossings: Design and Implementation", International Journal of Railway Technology, 5(2), 1-25, 2016. doi:10.4203/ijrt.5.2.1

1 Introduction

Railway turnouts are important elements of the railway infrastructure, which enable trains to be guided from one track to another at a railway junction as shown in Figure 1.

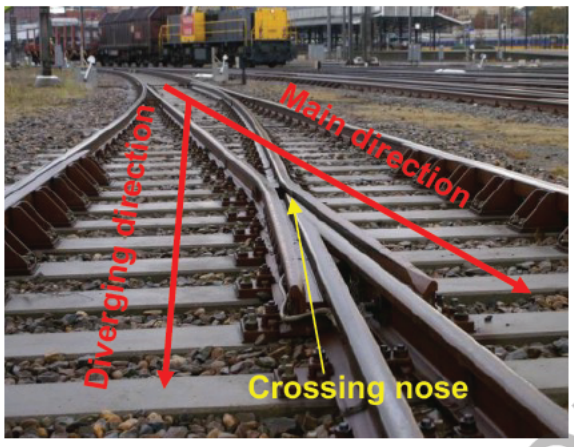

Figure 1 Railway turnout and crossing nos (red arrows show facing direction)

In this traditional crossing design th inner rail at the location of the crossing nose is discontinuous in both main and diverging directions as it can clearly be seen in Figure 1. Therefore, when passing the turnout in the facing direction (Figure 1) the railway wheel load has to be transferred from the wing rail to the crossing nose. The main stages of this process a e schematically shown in Figure 2.

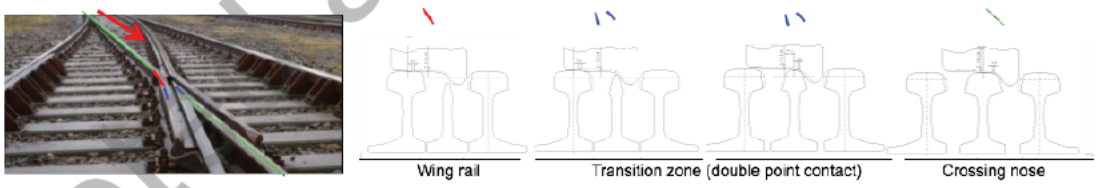

Figure 2 Wheel transition during travelling over crossing

Due o the rail discontinuity the crossing nose experiences high impact loads from the wheels of passing trains. The forces on the crossing nose can be extremely high when the trains travel in the main facing direction, since in this direction there is no speed restriction as compared to the divergent direction. These forces initiate various types of Rolling Contact Fatigue (RCF) damage (e.g. plastic deformations, shelling, spalling etc.) to the crossing nose of the railway turnout and wear (Figure 3). Increased RCF damage to the railway crossings is the major cause of operational disturbances in a railway network. In the Netherlands the situation is rather critical, so that every week two crossings need to be urgently repaired and annually around 300 crossings are to be replaced.

Figure 3 RCF damage to crossing nose

During the last decades analysis of the dynamic behaviour of railway crossings has been an active research area of the railway community. A number of numerical and experimental studies on the analysis of the vehicle-track interaction have been performed recently. Various numerical models for analysis of the dynamic behaviour of turnout have been developed, most of which are based on either the multibody (MB) or the finite element (FE) formalism e.g. [1]-[7]. The MB simulations are usually less time consuming than the FE simulations. Such simulations are usually used for the analysis of overall vehicle-turnout interaction, while the FE models are used for analysis of wheel-rail interaction to obtain stress-strain state in the contact area.

Experimental analysis of the turnout behaviour was initially performed for the purpose of numerical model validation e.g. [8], [9]. In [10] and [11] a mobile instrumented crossing device was used to assess performance of various turnout crossings and to determine the main factors influencing the crossing performance. The results of this study showed that geometry of the crossing has significant effect on the dynamic forces in turnout crossing and performance of the crossing can significantly be improved by adjusting of the crossing geometry e.g. by grinding during the maintenance.

Optimisation of railway turnouts (especially using the numerical optimisation methods) however has been performed not very often. As a continuation of the study performed in [4],[10] and [11] a method for numerical optimisation of the crossing geometry was proposed in [13] and [14]. The method combines the dynamic MB analysis for train-turnout interaction with numerical optimisation method. Other examples of the numerical optimisation of crossing geometry can be found in [15], [16]. Yet, in [15] the improvement of the crossing geometry was obtained simply by parameter variation (no optimisation method was used), while in [16] the assessment of the crossing design during the optimisation was based on only the kinematic analysis (no dynamic effects were taken into account).

In this study the optimisation procedure presented in [13] and [14] has further been developed. Based on the idea of adjusting the crossing geometry during maintenance by grinding, it is proposed to vary the location of the impact forces by adjusting the crossing geometry. By changing this location, the impact forces can better be spread along the crossing and the crossing nose material can better be used (loaded).

The goal of the optimisation considered here is improvement of crossing performance formulated as reduction of the RCF and wear indexes, while

controlling the location of wheel impact. The effect of two wheel profiles used on the considered crossing is taken in to account during the optimisation. In order to control the wheel transition location an extra constraint on the location of the wheel impact is introduced in the optimisation problem. Both changing the impact location and reduction of damage should result in prolonging of the operational life of the crossing. In order to implement the obtained improved geometry of the crossing a new measurement device has been developed.

The results of the experimental study that have inspired the presented optimisation are briefly described in Section 2. The numerical model used in the assessment of the dynamic behaviour of the turnout crossing is presented in Section 3. The multi-criteria optimisation problem is formulated in Section 4. The results of the optimisation and the implementation of the new crossing geometry are presented and discussed in Section 6.

2 Experimental study

Prior to the numerical optimization the dynamic interaction between the vehicle and turnout was analysed experimentally using the instrumented crossing device (ESAH-M), which consists of th following components (Figure 4a):

- The 3D acceleration sensor on a magnet which has to be placed at the side of the crossing nose (Figure 4b)
- Two inductive sensors to be installed on the rail in front of the crossing nose.
- The main unit, wherein all the signals are received, synchronised and analysed.

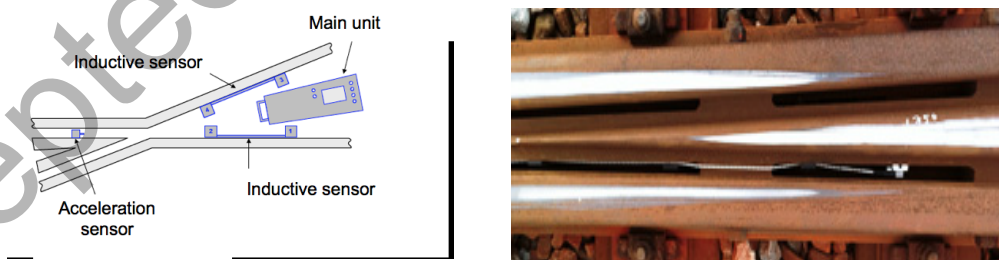

a. b.

Figure 4 Instrumented crossing (ESAH-M system): 3-D sensor on crossing nose (a) and schematic setup of ESAH-M (b)

The measurement data comprise of the crossing accelerations due to passing wheels (Figure 5a). Since the velocity of the passing train and the distance between the inductive sensors and the beginning of the crossing nose are known, it is possible to determine the maximum acceleration corresponding to each passing wheel of the train and location of this acceleration. The maximum acceleration corresponds to wheel impact. The locations of the wheel impacts are presented in a histogram (Figure 5b). The vertical axis in this histogram shows the percentage of the passed

wheels, while the horizontal axis shows the distance from the beginning of the crossing (point N) where the impact occurred. The location on the crossing where the most of the impacts occur is called fatigue area. So that in Figure 5b the fatigue area is approximately 25cm-50cm. The measured data on several turnouts wer collected and analysed in [10],[11].

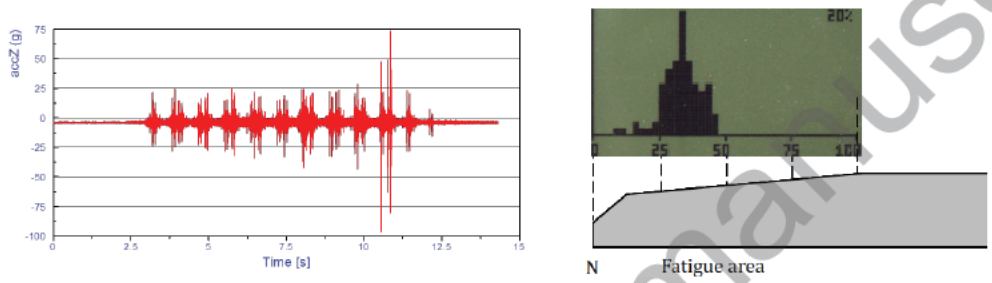

a. b.

Figure 5 Measurement results: crossing accelerations (a) and fatigue area of the crossing nose (b)

Performance of these turnout crossings was analysed based on the magnitude and location of the impacts of the wheels. At the same time the geometry of these crossings was obtained using a laser-based device (Figure 6a) by measuring the rail cross-sections in several locations along the crossing (Figure 6b).

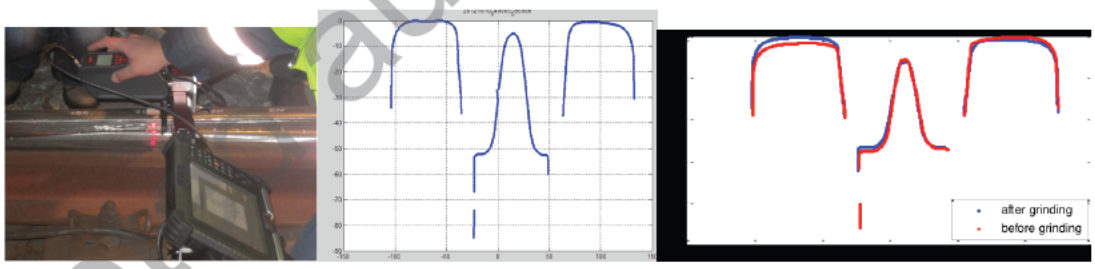

a. b. c.

Figure 6 Crossing geometry measurement device (a), cross-section profile: example (b) and effect of grinding (c)

Among the measured crossings there were newly laid, worn and repaired ones. The crossing repair is usually performed when a visible defect has been detected on the crossing nose. The repair process consists of removing the defect by cutting of the damaged material, adding new rail material by welding and restoration of the geometry by grinding the crossing and wing rails (Figure 7). Usually, the grinding is performed manually and the resulting crossing geometry to a great extent depends on the welder's skills and experience. Also, there is no special device to control the geometry during the grinding process. In order to improve the grinding process a new measurement device is proposed here (Section 6).

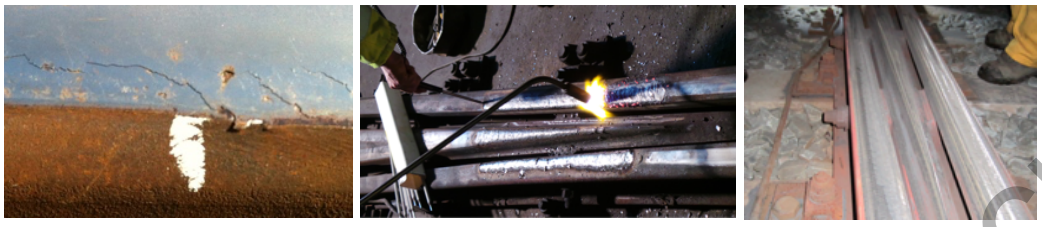

a. b. c.

Figure 7 Crossing repair process: RCF defect (a), adding new material after removing the defect (b), crossing after grinding (c)

The measurement results have shown that the crossing geometry has significant influence on the dynamic performance of the crossings. The changes in the geometry can affect both the location as well as the size of the fatigue area. So that, Figure 8 shows the geometry and the corresponding fatigue areas of two similar crossings (with the crossing angle 1:15 and the train speed 130 km/h). The crossings have different vertical geometry that was measured as the vertical distance between the wing rails and the crossing nose as shown in Figure 8a. The upper crossing was new (the measured and the theoretical geometries are very close) and the lower one wass repaired (the measured and the theoretical geometries differ significantly). From Figure 8b it can clearly be seen that the locations of the fatigue areas of these crossings are different, namely for the new crossing the fatigue area is located on the distance 0.40m-0.50m from the beginning of the crossing nose, while for the repaired crossing the fatigue area is located on the distance 0.6m-0.7m. The vertical axis in this figure is the percentage of the passed wheels.

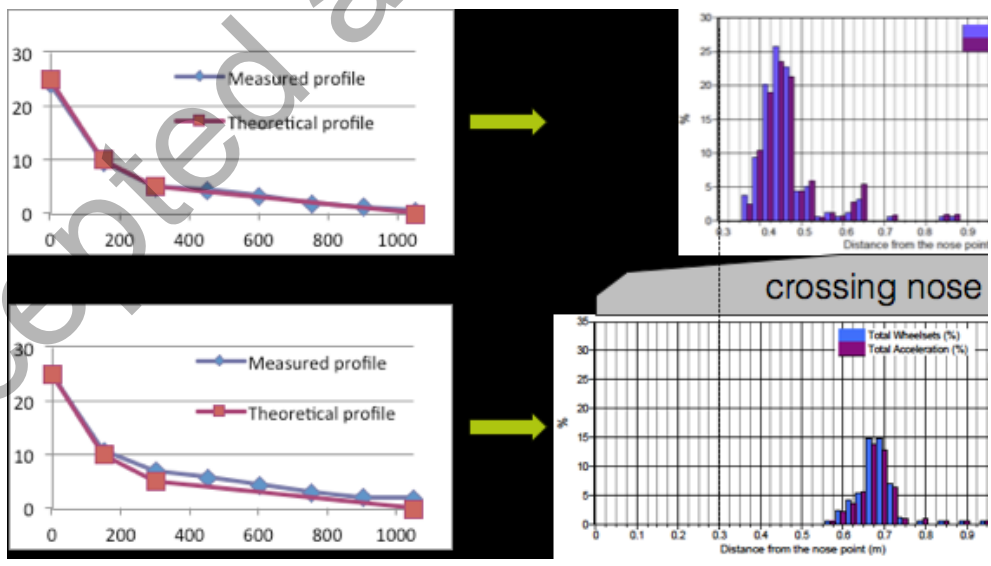

a. b.

Figure 8 Effect of crossing geometry on fatigue area: vertical distance between crossing nose and wing rails (a) and corresponding fatigue area (b)

Another example of the effect of the crossing geometry is given in Figure 9. The fatigue area on the crossing nose before the repair/grinding is in the range 0.5m-

0.6m, while after the grinding this area is much wider 0.4m-0.7m. It should be noted that the narrow fatigue area of the crossing before grinding has finally resulted in the fast developed (within 6 months) RCF deffect shown in Figure 7. After the repair, which was performed by an experienced welder the geometry of the crossing was changed (Figure 6c) and as a result only 30% of all the wheel impacts (496 wheels) were in the original fatigue area (0.5m-0.6m). The widening of the fatigue area can have a positive effect on damage reduction and prolonging the life of the crossing nose.

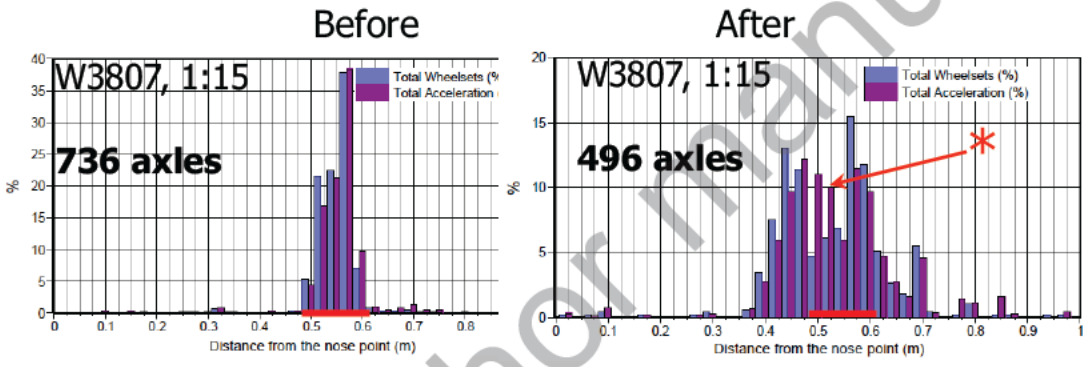

a. b.

Figure 9 Effect of repair/grinding (crossing angle 1:15, train speed 130 km/h): fatigue area before (a) and after repair (b)

These results have supported the idea of optimising the crossing geometry and implementing the improved geometry during the grinding process presented in [13], [14]. In this study, this idea has further been developed by stating that the performance (and ultimately life) of the crossing can significantly be improved by preventive grinding (not after appearance of the defects), while controlling the location of the wheel impacts (fatigue zone). In the forthcoming sections the optimisation procedure of the crossing aiming to improve crossing performance while a counting for the location of the fatigue area is presented.

3 Numerical model

In order to assess performance of various crossing geometries the dynamic model of the train-turnout system has been developed in the commercial MB package VI-Rail. The model is schematically shown in Figure 10. The parameters of the default vehicle model implemented in VI-Rail have been adjusted to meet the behaviour of the passenger intercity train of the VIRM type (the wheel load of 89 kN) used in the Netherlands. The track is represented using the 'moving track' model implemented in VI-Rail. In the 'moving track' model, the rails and sleepers are modelled as rigid bodies moving together with the wheel loads [17] as shown in Figure 10a. The wheel-rail contact forces are obtained using the FASTSIM algorithm.

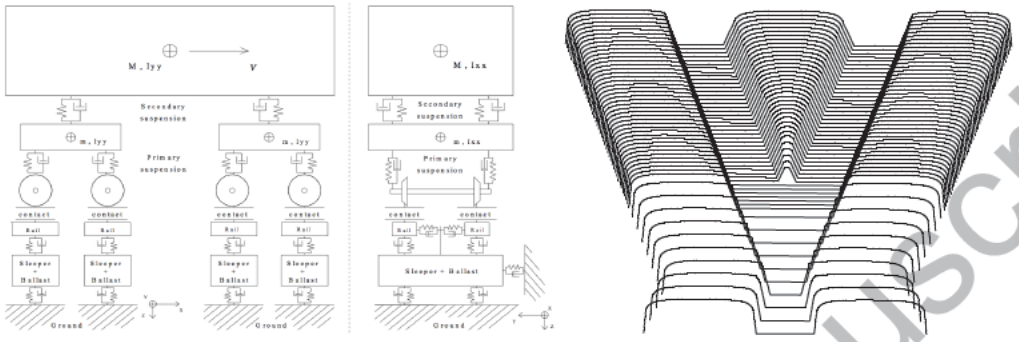

a. b.

Figure 10 Dynamic model (a) [12] and crossing geometry (b) developed in VI-Rail

In this study a turnout with the crossing angle of 1:15 (urve radius of 725 m) with the total length of 150 m has been modelled. The crossing geometry has been modelled using a number of the cross-sections as shown in Figure 10. In order to accurately calculate the contact forces the cross-sections with the smaller step were used in the crossing nose area. Details of the dynamic model used here can be found in [13].

During each simulation the train passes the turnout in the main facing direction with the speed of 140 km/h. After the simulation the responses such as the contact forces, creep forces, creepages etc. are obtained based on which performance of the crossing has been assessed and the design requirements have been checked. During the optimisation process multiple dynamic analysis were to be performed. The crossing assessment criteria and the design requirements used in the optimisation are described in the fo lowing sections.

4 Optimisation procedure

As it was mentioned earlier the goal of the optimisation was to improve the crossing performance via

- reducing the RCF damage and wear,
- controlling the location of wheel impacts to the crossing (fatigue area),

while satisfying other operational requirements (e.g. safety).

To achieve this goal the geometry of the crossing including the wing rails was varied.

In order to use the conventional non-linear mathematical programming methods the optimisation problem has to be formulated in the following general form

Minimize

$$F_0(\boldsymbol{x}) \quad \min, \quad \boldsymbol{x} \quad R^N \tag{1}$$

Subject to

$$g_j(\boldsymbol{x}) \quad 1, \quad j=1, \quad ,M \tag{2}$$

and

$$A_i \quad x_i \quad B_i, \quad i=1, \quad ,N \tag{3}$$

where F_0 is the objective function; g_j is the constraint; $\boldsymbol{x}$ is the vector of design variables; A_i and B_i are the side limits, which define lower and upper bounds of the *i*-th design variable.

The components of the vector $\boldsymbol{x}$ can represent various parameters of the mechanical system, such as geom try, load conditions, material properties, etc. The design variables are to be varied to improve the design performance. Depending on the problem under onsideration, the objective and constraint functions (1)-(2) can describe various structural and dynamic response quantities such as weight, reaction forces, stresses, strain, natural frequencies, displacements, velocities, accelerations, etc. The objective function provides a basis for design improvements.

To solve the optimisation problem (1)-(3) the Multipoint Approximation Method (MAM) was employed. The method uses the mid-range approximations instead of the o iginal functions to reduce the computational cost of the optimisations. MAM does not require the design sensitivity information though it can effectively be taken into account if available. Moreover the optimisation method can easily be coupled with any response analysis software. More details of MAM can be found in [18]-[19].

4.1 Design variables

As it was mentioned earlier in this paper, improvement of the crossing performance is achieved by varying the crossing geometry. In order to use the numerical optimisation method the vector of the design variables in (1)-(3) should be defined based on some parameterisation of the crossing geometry. Here the crossing geometry parameterisation proposed in [23] was used, which is briefly presented below.

According to the current manufacturing process of the crossings and also the standard of ProRail (the Dutch rail infra-provider) the crossing geometry is defined by the 4 cross-sections located on the distances 0, 10xA, 20xA and 70xA from the tip point (TP) of the crossing, where A is equal to the crossing angle in mm (here A=15mm) as it is shown in Figure 11.

(a)

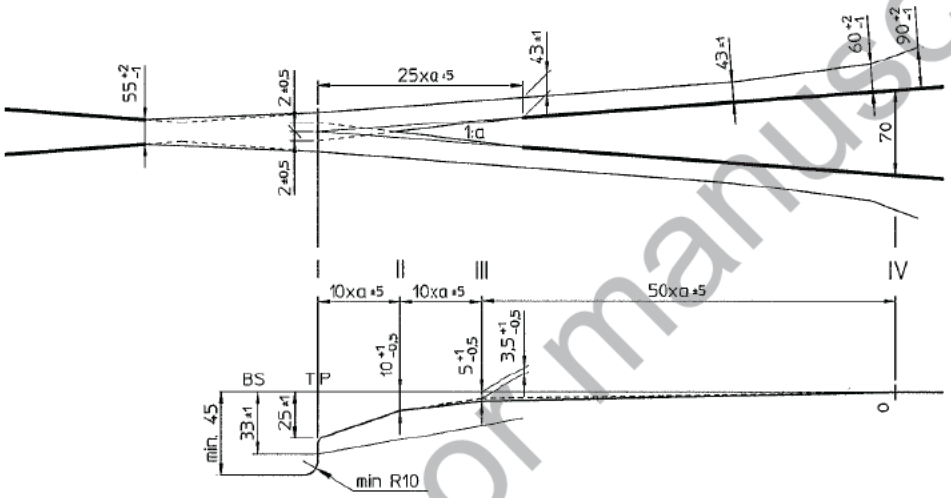

Figure 11 Crossing geometry: Top view (a), longitudinal profile of crossing nose (b)

To vary the crossing geometry an additional cross-section is introduced at the distance of 40xA from TP, so that the longitudinal profile of the crossing nose is defined by 5 cross-sections as it is shown in Figure 12a . The heights of the cross-section III and V are chosen as the design variables x1 and x2 (Figure 12a). Each cross-section is approximated by a cubic B-spline with 6 control points, whereas the position of the control point P3 is chosen as the design variable x3 (Figure 12b). The B-spline app oximation has been successfully used in optimising the wheel profiles [20][21] and crossing nose profiles [16]. One of the advantages of a B-spline (of the k-th order with n+1 control points) is that each control point affects only k segments of the B-spline among its $n - k + 2$ segments, which gives global rather than local control of the shape of the B-spline [13]. Definition and exact location of the control points is given in [23].

Based on the manufacturing process of crossings with raised wing rails, the wing rail is raised before TP. A schematic drawing of the wing rail raised to the level d (above the top of the normal rail) is shown in Figure 12c. To achieve the vertical level d, the wing rail is bent over the location $L1$–$L2$ before TP. Starting from $L2$, the height of the rail reaches the designed level. Usually, the values of the parameters $L1$ and $L2$ depend on the height of the wing rail d. Here, the values $L1$ = 1225 mm and $L2$ = 225 mm, corresponding to d = 3 mm taken from the manufacturer, are used. For simplicity, these values are not changed when adjusting the value of d. The design variable x4 =d has been chosen to control the height of the wing rail (Figure 12c).

In total, 4 design variables are selected to vary the geometry of the crossing and the wing rails. More details on the parameterisation of the crossing geometry can be found in [23].

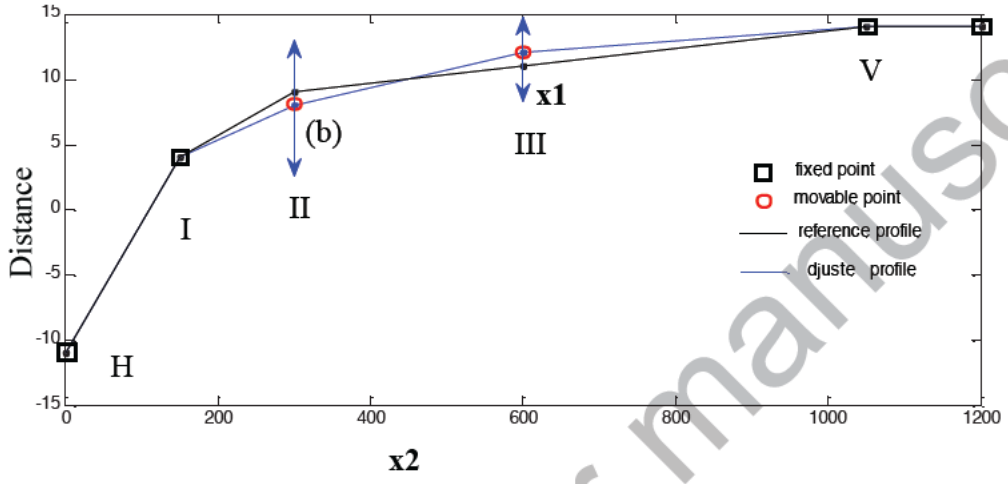

a.

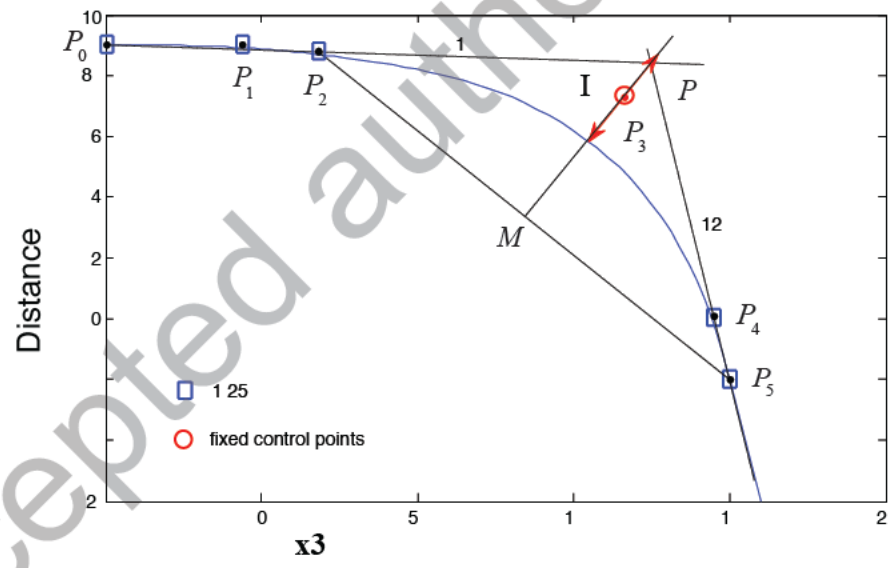

b.

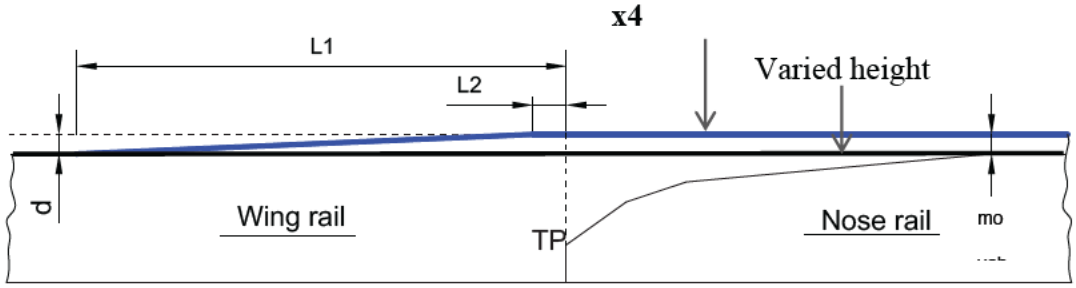

c.

Figure 12 Design variables: Crossing nose longitudinal - x1, x2 (a) and lateral - x3 (b) profiles; Wing rail height – x4 (c)

4.2 Performance criteria

As it was mentioned in the previous Sections the main goal of the optimisation was improving the crossing performance, while controlling the location of the fatigue area on the crossing nose. Below, the definition of these requirements and their use in the formulation of the optimisation problem are described.

4.2.1 Damage indicators

The criteria of the optimisation is reduction of damage to crossing and wear, which in the presented study are estimated by the normal contact pressure S and the energy dissipation W at the wheel-rail contact patch along the crossing. The contact pressure is related to the plastic deformation type of failure and here estimated as [24]:

$$S(t) = \frac{3}{2}\frac{F_n(t)}{A(t)} \tag{4}$$

where F_n is the normal contact force, and A is the size of the contact patch. The wear index based on the energy dissipation is evaluated using the T criterion according to [25]:

$$W(t) = \left|F_x(t)\ \ _x(t)\right| + \left|F_y(t)\ \ _y(t)\right| \tag{5}$$

where F_x and F_y are the creep forces in the longitudinal and lateral direction, respectively; $_x$ and $_y$ are the corresponding creepages obtained from the dynamic simulation of the train travelling over the turnout.

The time histories of these damage indicators obtained for the wheel S1002 and the crossing (1:15) are shown in Figure 13. The solid and dotted lines in this figure correspond to the responses on the wing rail and the crossing nose respectively.

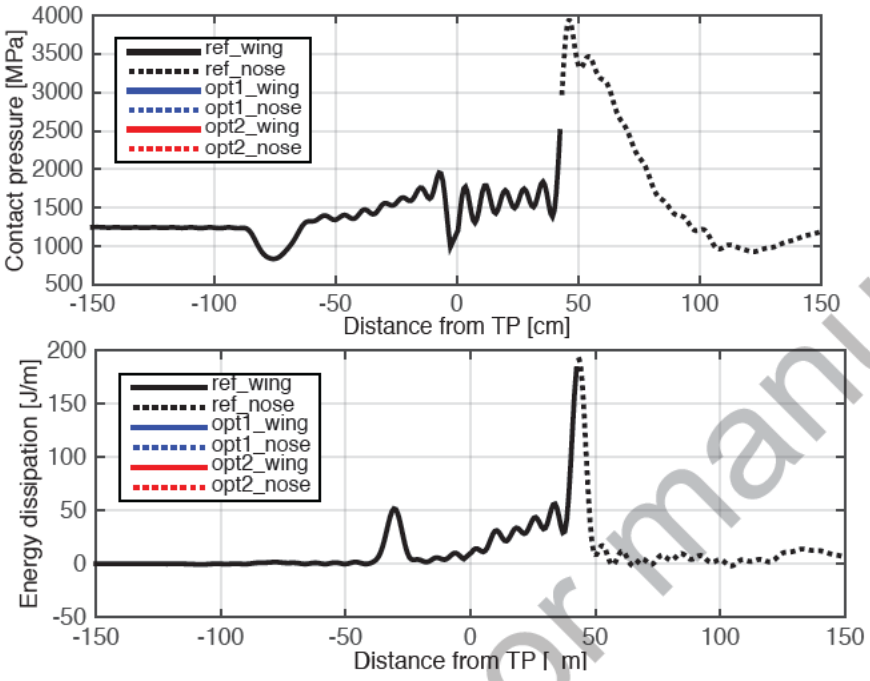

Figure 13 RCF and wear indicators for assessment of crossing performance (wheel S1002)

In order to use these response quantities in the optimisation problem (1)-(3) the time dependence in these indicators has to be removed. Here, it is achieved by using the equivalent cumulative representation in the form of Kresselmeier-Steinhauser function [19] that reads:

$$\bar{S}(\boldsymbol{x}) = \frac{1}{} \ln \sum_{i=1}^{T} e^{S(\boldsymbol{x},t_i)/S_{\max}(\boldsymbol{x})} \quad S_{\max}(\boldsymbol{x}) \tag{6}$$

$$\bar{W}(\boldsymbol{x}) = \frac{1}{} \ln \sum_{i=1}^{T} e^{W(\boldsymbol{x},t_i)/W_{\max}(\boldsymbol{x})} \quad W_{\max}(\boldsymbol{x}) \tag{7}$$

where

$$S_{\max}(\boldsymbol{x}) = \max(S(\boldsymbol{x},t_i)), \quad i = 1,\ldots,T \tag{8}$$

$$W_{\max}(\boldsymbol{x}) = \max(W(\boldsymbol{x},t_i)), \quad i = 1,\ldots,T \tag{9}$$

Here, T is the total number of the time points during one simulation. The parameter μ determines the discrepancy between $\bar{S}$ ($\bar{W}$) and the most critical value S_{max} (W_{max}). In the present paper μ equal to 50 is used in all KS functions (6)-(7). More detailed explanation of the KS function can be found in [19].

In order to obtain robust crossing geometry two typical wheel profiles (S1002 and HIT) that are used on the considered railway line have been used here to assess the performance of the crossing during the optimisation (Figure 14). In order to increase the robustness of the opimised crossing a wider variation of the wheel profiles should be considered as e.g. in [16]. Due to the lack of the measuremen data only 2 wheel profiles were used in this study. Because of the well-organised re-profiling regime of the wheels of the trains on the considered line the variation in the wheel profiles is minimal. Therefore, these 2 profiles cou d be considered as the representative ones.

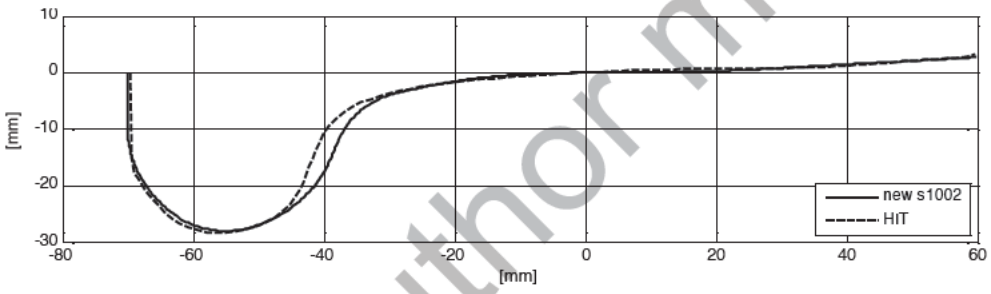

Figure 14 Representative wheel profiles of VIRM trains: S1002 and HIT

Thus, the objective function formulated as the weighted sum of the response quantities obtained from the dynamic simulations with these two wheel profiles is used here, which reads:

$$F_0(\boldsymbol{x}) \quad w_1 \sum_{i=1}^{d} {}_i \frac{\bar{S}_i(\boldsymbol{x})}{\bar{S}_i} + w_2 \sum_{i=1}^{d} {}_i \frac{\bar{W}_i(\boldsymbol{x})}{\bar{W}_i} \qquad \min, \tag{10}$$

The normalising factors $\bar{S}$ and $\bar{w}^*$ in (10) are the cumulative contact pressure (6) and wear index (7) corresponding to the reference situation. w_1 and w_2 are the weight coefficients ($w_1 + w_2 = 1$, d=2). Considering the fact that the HIT profile (the 2nd wheel) is more commonly used than the s1002 profile (the 1st wheel), the weight coefficient pair $[\ {}_1,\ {}_2] = [0.25, 0.75]$ is applied. Since the RCF defects (plastic deformations) are the most damaging ones for the crossings, wear index reduction was not considered here, i.e. $w_2 = 0$, while the wear index was still calculated for each intermediate design during the optimisation.

It should be noted that the objective function formulation (10) can easily be adjusted in case of wider variation of the system parameters in the optimisation, such as different wheel profiles, type of rolling stock or track properties etc. by including additional weighted components (d>2).

4.2.2 Location of fatigue zone

In Section 2 it was shown that when the fatigue area is relatively narrow and its location does not change, it could result in fast development of the RCF defects (Figure 7a). By changing the location of the fatigue zone, the bigger part of the crossing can be used for wheel contact and therefore the life of the crossing can be prolonged.

Here, the fatigue zone (Section 2) is defined by the location of the maximum normal pressure, which is in the reference situation (wheel S1002) around 50 cm from the TP (Figure 13). In order to control the location of the fatigue area, the constraint on the location of the maximum contact pressure has been imposed. In the first optimisation the location was prescribed by the range 25cm – 45 cm from the TP, while in the second optimisation the range 45mm – 65cm from TP was used (Figure 15).

4.3 Other constraints

Apart from the above-mentioned constraints on the location of the fatigue zone a number of additional constraints have been imposed. The wheel-rail contact on the crossing nose in the area A (0-25cm from TP) and on the wing rail in the area C (65mm from TP) was not allowed. These areas are schematically shown in Figure 15.

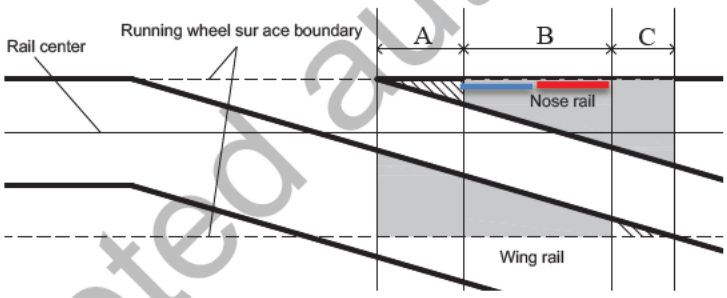

Figure 15 Wheel transition over crossing and locations of fatigue areas (blue line – optimisation 1 and red line – optimisation 2)

Additionally, a number of geometrical constraints have been imposed to prevent unrealistic shapes of the crossing. In order to prevent derailment the location of the contact point on the wheel was controlled, so that the contact in the 'danger zone' (the thick red line) as it is shown in Figure 16 was not allowed.

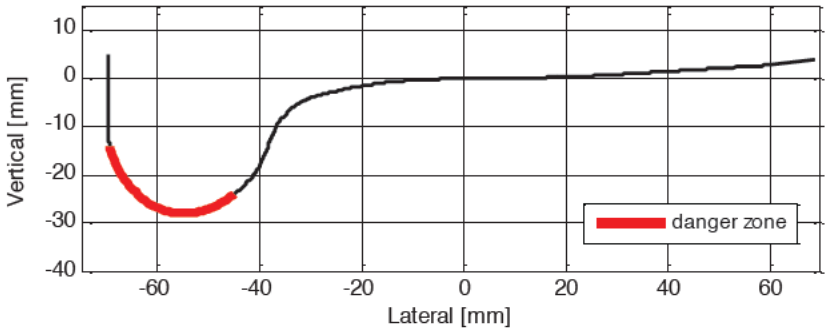

Figure 16 Derailment zone on wheel profile

5 Results and discussion

Using the formulation (1)-(3) and the objective and constraint functions described in Section 4 two optimisation problems have been formulated and solved. In the first optimisation problem (the corresponding results are denoted as 'opt1') the fatigue zone was restricted by 25cm-45cm, while in the second optimisation (the corresponding results are denoted as 'opt2') the fatigue zone was restricted by 45cm-65cm. The results of both optimisations and the reference situation (the corresponding results are denoted as 'ref') are shown below.

5.1 Optimised crossings

In Figure 17 the changes in the crossing profiles in the optimum designs are shown. The dashed lines in this figure correspond to the wing rail and the solid line - to the crossing nose. As it can be seen from Figure 17 the height of the wing rail is reduced in the optimum crossing design. This is in agreement with the results of the parametric study presented in [14].

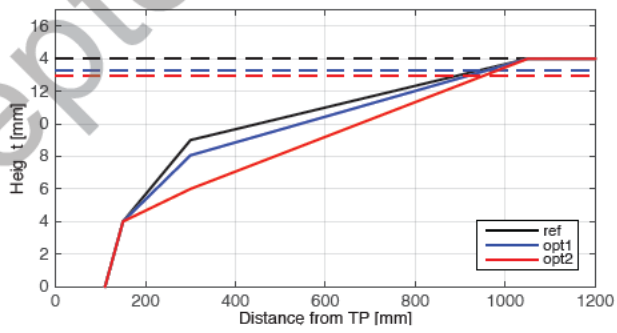

a.

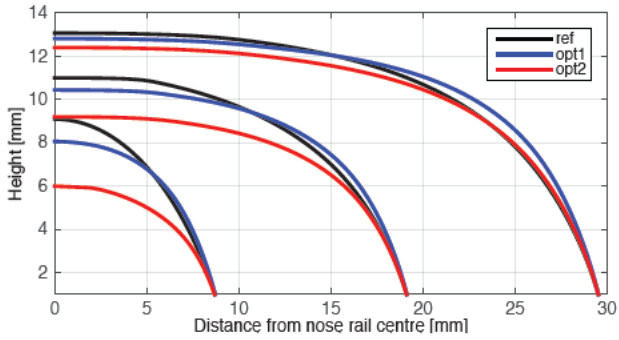

b.

Figure 17 Optimised crossings: longitudinal (a) and lateral (b) profiles

From Figure 17, it can also be seen that the shape of th crossings 'opt2' is located inside the shape of the crossing 'opt1' (i.e. all the blue lines are above the red lines), which means that the geometry of the crossing 'opt2' can be obtained by adjusting of the geometry of the crossing 'opt1' e.g. by grinding. When changing the crossing shape in the order 'opt1'->'opt2' the fatigue area is also shifting along the crossing nose further from TP (according to the defini ion of the optimisation problem). By shifting the fatigue area to the region 45cm 65cm, it is possible to obtain stress relief in the region 25cm-45cm.

The changes in performance of the optimised crossings are presented in Figure 18 and Figure 19. As it can be seen from these figures for both wheel profiles the magnitude of the maximum contact pressure (the RCF index) is reduced and the location of its maximum value (the fatigue area) is changed according to the definition of the optimisation problem. These results show that the optimisation method has succeeded to find the optimum solution according to the formulated criteria.

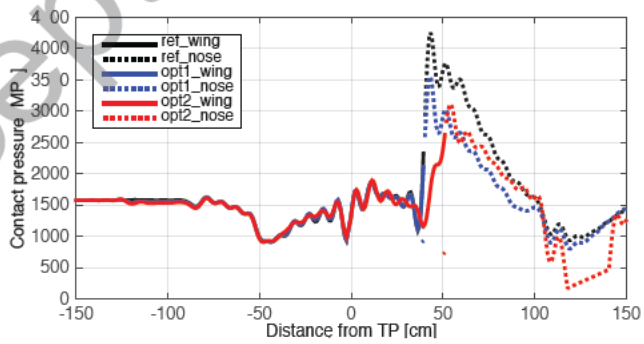

a.

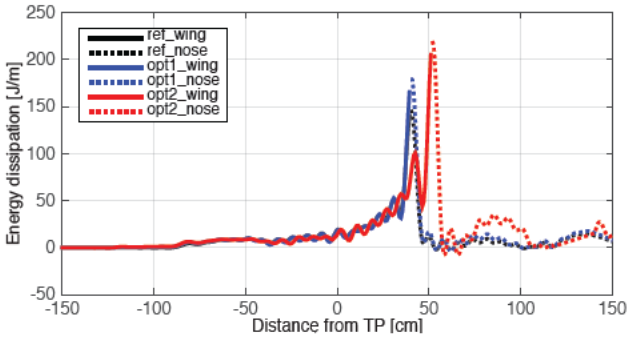

b.

Figure 18 Optimum crossing performance changes for HIT wheel profile: RCF (a) and wear indexes (b)

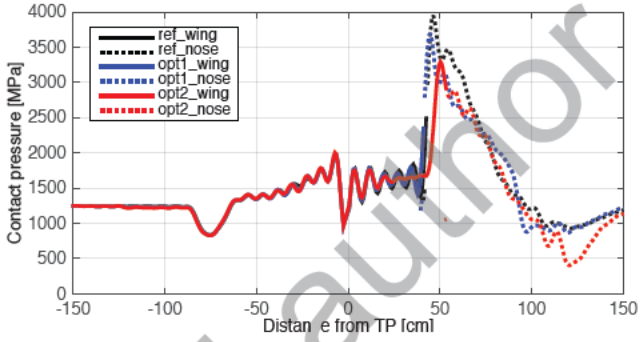

a.

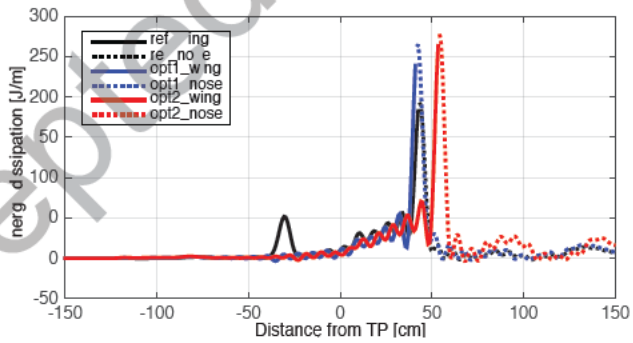

b.

Figure 19 Optimum crossing performance changes for S1002 wheel profile: RCF (a) and wear indexes (b)

5.2 Robustness check

In order to assure the robustness of the obtained crossings, their performance was checked using the dynamic simulations (Section 2) with the lateral and vertical irregularities [23]:

- *irr_1*: the vertical deviation in the rail geometry of 8 mm over 10 m at the crossing side (Figure 20a), which commonly occurs if tamping maintenance at the crossing is not performed in time.
- *irr_2*: the lateral serpentine deviation of the rail with wavelength 12 m and amplitude 5 mm at the stock rail side of the crossing panel, starting from 16 until 4 m before the nose point (Figure 20a). Such irregularities can occur, for instance, due to damaged fastening system on one side of the track.

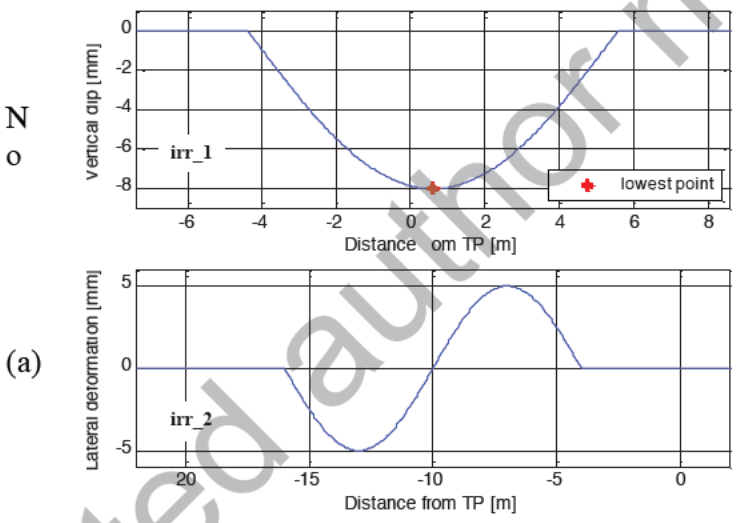

(a)

Figure 20 Track irregularities in robustness analysis: (a) vertical and (b) lateral

The performance results of the optimised crossings for the S1002 and HIT wheel profiles are shown in Figure 21 and Figure 22. From these figures it can be seen that the maximum contact pressure for the optimised crossings is still reduced as compared with the reference crossing. The location of the maximum contact pressure that reflects the fatigue area is also within the chosen limits.

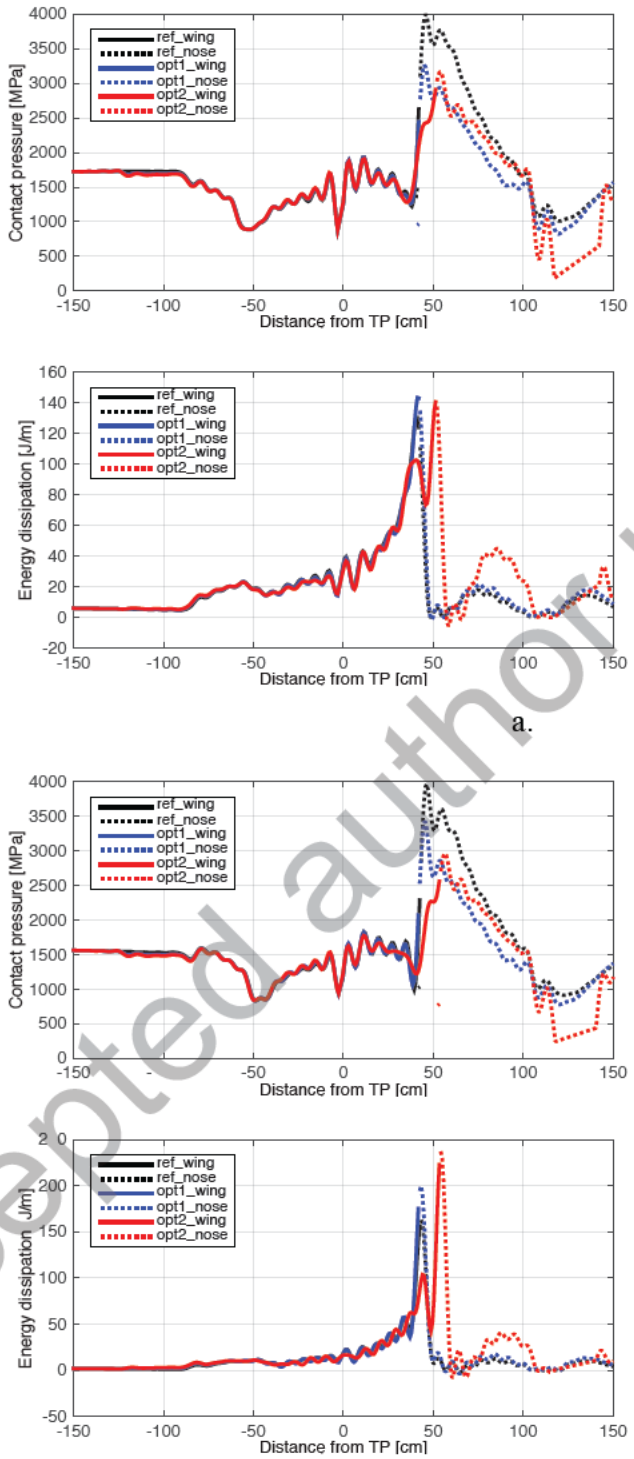

a.

b.

Figure 21 Robustness performance check of optimised crossings for HIT wheel profile using lateral (a) and vertical (b) track irregularities

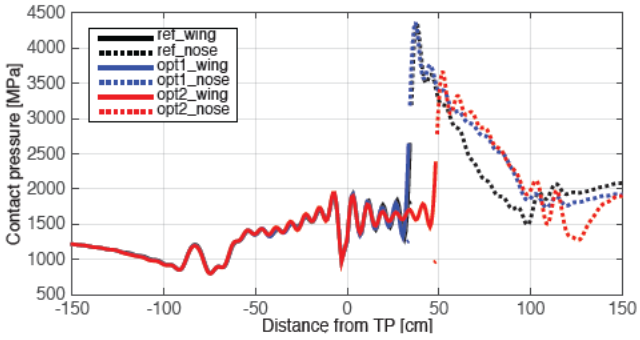

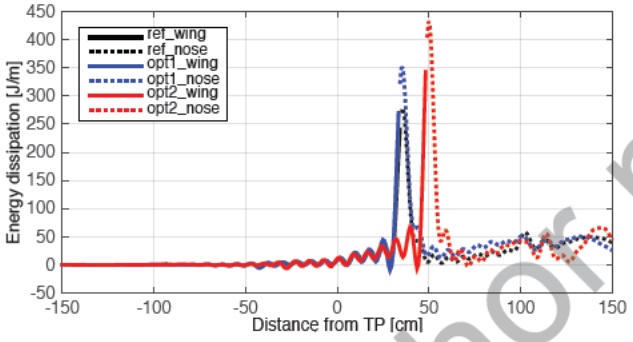

a.

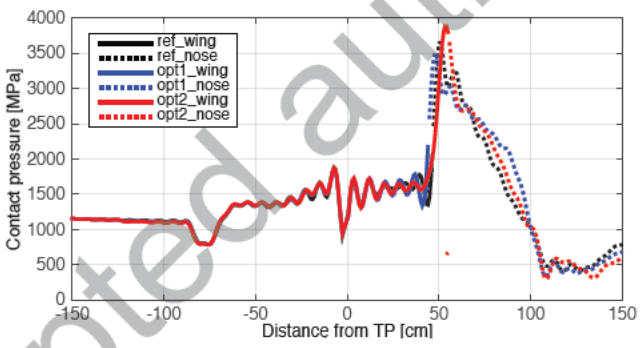

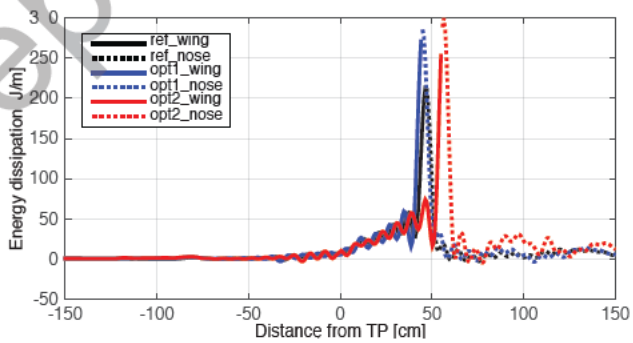

b.

Figure 22 Robustness performance check of optimised crossings for S1002 wheel profile using lateral (a) and vertical (b) track irregularities

6 Implementation of new geometries

The results of the optimisation presented in the previous Section have shown that the performance of the crossing can be improved by using the optimisation procedure (Section 4). Also, it was shown that the optimised crossing geometries can be achieved by grinding.

In order to accurately implement the improved crossing geometry a new device has been developed. This device can be used for assessment/controlling of the shape (geometry) of a railway crossing. The geometry can be controlled both during inspection and during maintenance (grinding) of the crossings.

Usually, the geometry of a crossing is assessed visually by using a rigid bar (2m) or by measuring separate cross-sections of the crossing nose in 2 locations. In the proposed device the templates of the several cross-sections of the crossing and wing rails are connected to a rigid bar, so that the shape of the whole frog including the wing rails can be controlled.

The prototype of the device is shown in Figure 23. The templates correspond to the cross-sections of the crossing including the wing rails, which are evenly spread along the length of the crossing. The shapes of the templates are automatically obtained from the 3-D shapes of the crossings using AutoCAD and Matlab software. The templates for other crossing geometries can easily be obtained by changing the 3-D shape of the crossing.

Using the same procedure the device can easily be adjusted for the crossings of different crossing angle, e.g. 1:9. In this case the number of the templates and the distance between the templates are to be adjusted.

Figure 23 Crossing geometry measurement device

The device can be used for assessment of wear of the existing crossings. By analysing the discrepancies (voids) between the templates and the rail surface the deviations between the designed (device) and actual crossing geometry can easily be detected. Also, during the maintenance this device can be used to control the grinding process.

By changing the templates the device can be adjusted for various crossing geometries. So that, the devices for the reference, ‘opt1’ and ‘opt2’ crossings from

this study have been built. The next step in this study is to implement these geometries and to verify performance of the obtained crossing.

7 Conclusions

In this paper an optimisation procedure for improvement of crossing performance by adjusting the crossing (including the wing rail) geometry is presented. Improvement of the crossing performance is achieved by reducing the RCF damage (plastic deformations) and wear indexes, which were estimated numerically by the normal pressure and energy of dissipation in wheel-rail contact respectively.

Using the idea of adjusting the crossing geometry during maintenance by grinding, it was proposed to control the location of the wheel imp ct during the optimisation procedure. By shifting the fatigue area during the maintenance (grinding) the life of the crossing can be prolonged.

To demonstrate the proposed procedure the geometry of a 1:15 crossing has been optimised. To assure the robustness of the improved crossing, two typical wheel profiles used on the considered crossing were taken into account during the optimisation. The results have shown that the reduction of the contact pressure and changing of the location of the wheel impact (fatigue area) on the crossing can be achieved by using the proposed optimisation procedure. The robustness of the obtained geometries has been verified using the numerical simulations with track geometrical irregularities.

Using the optimisation procedure two improved geometries of the crossing have been obtained. In both designs the RCF damage index was reduced as compared to the reference design. At the same time, the fatigue area in the second crossing was shifted further from the tip point along the crossing nose as compared to the first optimised crossing. It should be emphasised that the second optimised crossing geometry can be obtained by adjusting the geometry of the first optimised crossing e g. by grinding.

To implement the new crossing geometry (including the crossing nose) a new measurement device has been proposed. The device can be used for both assessment and during adjusting/restoration of the crossing geometry. The proposed device can easily be adjusted for various crossing geometries and different crossing angles.

The next step in this research will be implementation and validation of the obtained crossing geometries.

References

[1] E. Kassa, C. Andersson and J.C.O. Nielsen, “Simulation of dynamic interaction between train and railway turnout”, Vehicle System Dynamics, March 2006, Vol. 44, No.3, pp. 247-258.

[2] M. Wiest, W. Daves, F.D. Fischer and H. Ossberger, "Deformation and damage of a crossing nose due to wheels passages", Wear, Vol. 265, pp. 1431-1438.

[3] S. Alfi and S. Bruni, "Mathematical modelling of train-turnout interaction", Vehicle System Dynamics, 47:5, 551- 574.

[4] V.L. Markine, M.J.M.M. Steenbergen and I.Y. Shevtsov, "Combatting RCF on switch points by tuning elastic track properties", Wear 271 (2011), pp. 158-167. doi:10.1016/j.wear.2010.10.031

[5] C. Wan, V.L. Markine and I.Y. Shevtsov, Simulation of Train-Turnout Interaction and Validation using Field Measurements. In Proceedings of the First International Conference on Railway Technology: Research, Development and Maintenance, J. Pombo, (Editor), Civil-Comp Press, Stirlingshire, United Kingdom, paper 136, 2012. doi:10.4203/ccp.98.136

[6] Xin, L., V.L. Markine, and I.Y. Shevtsov, Dynamic Interaction Between the Wheel and Crossing Nose, *in Proceedings of the Fourteenth International Conference on Civil, Structural and Environmental Engineering Computing, B.H.V. Topping and P. Iványi, Ed tors* 2013, Civil-Comp Press, Stirlingshire, United Kingdom. paper 22

[7] Xin, L., V.L. Markine, and I.Y. Shevtsov, Simulation of Railway Crossing Damage Due to Welding Defect, in Railway Technology: Research, Development and Maintenance (Railways2014), J. Pombo, Editor. 2014, Civil-Comp Press: Ajaccio, France.

[8] Kassa, E. and J.C.O Nielsen, *Dynamic interaction between train and railway turnout: full scale field test and validation of simulation models.* Vehicle System Dynamics, 2008. **46**: p. 521-534.

[9] Wan, C., V.L. Markine, and I.Y. Shevtsov, Analysis of train/turnout vertical interaction using a fast numerical model and validation of that model. *Proceedings of the Institution of Mechanical Engineers Part F-Journal of Rail and Rapid Transit*, 2014. **228**(7): p. 730-743.

[10] Markine, V.L. and Shevtsov, I.Y. (2012) Experimental Analysis of the Dynamic Behaviour of Railway Turnouts. In Topping, B.H.V., ed. *The Eleventh International Conference on Computational Structures Technology* (Civil-Comp Press, Dubrobnik, Croatia, 2012).

[11] Markine, V. L. and Shevtsov, I. Y. (2013) An Experimental Study on Crossing Nose Damage of Railway Turnouts in The Netherlands. In Proceedings of the Fourteenth International Conference on Civil, Structural and Environmental Engineering Computing (CC2013), 2013, pp. paper 37.

[12] Bezin Y. An integrated flexible track system model for railway vehicle dynamics. PhD thesis. Manchester Metropolitan University. Manchester, UK. 2008. ISBN 978-1-905476-42-8.

[13] C. Wan, V.L. Markine, and I.Y. Shevtsov, "Improvement of vehicle–turnout

interaction by optimising the shape of crossing nose", Vehicle System Dynamics, 2014. **52**(11): p. 1517-1540.

[14] Wan C, Markine VL, Dollevoet RPBJ. Robust optimisation of railway crossing geometry. *Vehicle System Dynamics*. 2016; in pr ss. doi: 10.1080/00423114.2016.1150495. .

[15] Ren R, Sun S, Xie G. A method to determine the two-point contact zone and transfer of wheel-rail forces in a turnout. Veh Syst Dyn. 2010; 48(10): 1115-1133.

[16] Pålsson BA. Optimisation of railway crossing geometry considering a representative set of wheel profiles. Veh Syst Dyn. 2015; 53(2): 274-301.

[17] VI-Rail 16.0 Documentation, VI-grade GmbH, 20 3

[18] Toropov VV. Simulation approach to structur l optimization. Structural Optimization. 1989; 1(1):37-46.

[19] Markine, V.L. (1999) Optimisation of the dynamic behaviour of mechanical systems. PhD thesis, Delft University of Technology. ISBN 90-423-0069-8

[20] Markine, V.L., I.Y. Shevtsov, and C. Esveld, *An inverse shape design method for railway wheel profiles* Structural and Multidisciplinary Optimization, 2007. **33**(3): p. 243-253.

[21] Markine, V.L. and I.Y. Shevtsov, *Optimization of a wheel profile accounting for design robustness*. Proceedings of the Institution of Mechanical Engineers Part F-Journal of Rail and Rapid Transit, 2011. **225**(F5): p. 433-441.

[22] Brabant, V and C. Fleury, *Shape optimal design usin B-splines.* Computer Methods in Applied Mechanics and Engineering, 1984(44): p. 247-267.

[23] Wan C. and V.L. Markine, Parametric study of wheel transitions at railway cross ngs. *Vehicle System Dynamics*, 2015. **53**(12): p. 1876-1901.

[24] Ekberg A, Kabo E, Andersson H. An engineering model for prediction of rol ing contact fatigue of railway wheels, Fatigue and fracture of engineering materials and structures, 2002, vol. 25(10), pp. 899-909.

[25] Kalker JJ. Three-dimensional elastic bodies in rolling contact. Dordrecht: Kluwer Academic Publishers; 1990.